Copolymerization of Polythiophene and Sulfur To Improve the Electrochemical Performance in Lithium–Sulfur Batteries

ARTICLE *in* CHEMISTRY OF MATERIALS · OCTOBER 2015

Impact Factor: 8.35 · DOI: 10.1021/acs.chemmater.5b02317

CHEMISTRY OF MATERIALS

Article

pubs.acs.org/cm

Copolymerization of Polythiophene and Sulfur To Improve the Electrochemical Performance in Lithium−Sulfur Batteries

Bernd Oschmann,[†,‡,#] Jungjin Park,[§,∥,#] Chunjoong Kim,[⊥] Kookheon Char,[§] Yung-Eun Sung,[*,§,∥] and Rudolf Zentel[*,†]

[†]Institute for Organic Chemistry, Johannes Gutenberg University, Duesbergweg 10-14, D-55128 Mainz, Germany

[‡]Graduate School of Excellence "Materials Science in Mainz", Johannes Gutenberg University, Staudinger Weg 9, D-55128 Mainz, Germany

[§]School of Chemical and Biological Engineering, The World Class University Program of Chemical Convergence for Energy and Environment, The National CRI Center for Intelligent Hybrids, Seoul National University, Seoul 151-744, Korea

[∥]Center for Nanoparticle Research, Institute for Basic Science, Seoul National University, Seoul 08826, Korea

[⊥]Materials Science and Engineering, Chungnam National University, Daejon 305-764, Korea

Supporting Information

ABSTRACT: We first report on the copolymerization of sulfur and allyl-terminated poly(3-hexylthiophene-2,5-diyl) (P3HT) derived by Grignard metathesis polymerization. This copolymerization is enabled by the conversion of sulfur radicals formed by thermolytic cleavage of S_8 rings with allyl end-group. The formation of a C−S bond in the copolymer is characterized by a variety of methods, including NMR spectroscopy, size exclusion chromatography, and near-edge X-ray absorption fine spectroscopy. The **S-P3HT** copolymer is applied as an additive to sulfur as cathode material in lithium−sulfur batteries and compared to the use of a simple mixture of sulfur and P3HT, in which sulfur and P3HT were not covalently linked. While P3HT is incompatible with elementary sulfur, the new **S-P3HT** copolymer can be well dispersed in sulfur, at least on the sub-micrometer level. Sulfur batteries containing the **S-P3HT** copolymer exhibit an enhanced battery performance with respect to the cycling performance at 0.5C (799 mAh g^{-1} after 100 cycles for **S-P3HT** copolymer versus only 544 mAh g^{-1} for the simple mixture) and the C-rate performance. This is attributed to the attractive interaction between polysulfides and P3HT hindering the dissolution of polysulfides and the charge transfer (proven by electrochemical impedance spectroscopy) due to the homogeneous incorporation of P3HT into sulfur by covalently linking sulfur and P3HT.

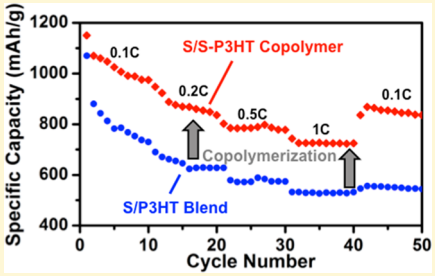

INTRODUCTION

Currently, Li-ion rechargeable batteries are considered promising energy storage devices to tackle problems related to the use of renewable energy instead of fossil fuels.[1] However, Li-ion batteries that commonly contain graphite as an anode and lithium cobalt oxide as a cathode material are limited with regard to their specific capacity and energy density. In addition, cobalt-containing materials are neither economically nor environmentally friendly. To meet the extensively growing demand for high-energy storage devices for electric vehicles, energy storage systems, and biomedical equipment, it will be necessary to substitute the currently used electrode materials in a timely manner. The lithium−sulfur battery, with a theoretical specific energy more than 6 times higher than that of the current Li-ion battery, is one of the most promising candidates to solve these issues. In addition, sulfur is a very abundant, cheap, and nonharmful material.[2−4]

However, lithium−sulfur batteries still suffer from several issues, including the insulating nature of sulfur, volume expansion during cycling, and unique reaction processes (dissolution/precipitation of active material during (de)-lithiation and the so-called "shuttle" mechanism, etc.).[2,5,6] These cause capacity decay by irreversible loss of reaction species and/or sites as cycles are repeated. So far, several approaches have been introduced to increase the electrical conductivity and prevent the loss of the soluble polysulfides. These include the use of conductive polymer coating or the encapsulation of sulfur with various carbonaceous materials such as mesoporous carbon, hollow carbon particles, carbon nanotubes, and graphene-based materials.[7−17] Other approaches are based on the use of polysulfide-adsorbing additives, which trap the polysulfides.[18−20] Recently, an experimentally simple approach based on inverse vulcanization has been introduced. It uses 1,3-diisopropenylbenzene (DIB) for radical copolymerization with a molten sulfur radical species, resulting in synthesis of polymeric sulfur materials which exhibited an improved battery performance compared to pure sulfur.[21−23] Extension of this approach to a tandem inverse

Received: June 19, 2015
Revised: October 5, 2015

DOI: 10.1021/acs.chemmater.5b02317
Chem. Mater. XXXX, XXX, XXX−XXX

vulcanization resulted in an electropolymerization-derived polythiophene incorporated in a sulfur−DIB copolymer with reduced charge-transfer resistance.[24] However, a detailed study of the structure and chain length of the resulting oligo- or polythiophenes is not yet reported. Furthermore, this composite material contains a relatively low sulfur loading (50 wt.% after inverse vulcanization), which limits its capacity.

Herein, we introduce the first copolymerization of well-defined allyl-terminated poly(3-hexylthiophene-2,5-diyl) (P3HT) synthesized by Grignard metathesis (GRIM) polymerization with an excess of molten sulfur radicals, resulting in the **S-P3HT** copolymer. This **S-P3HT** allows the homogeneous incorporation of a well-defined semiconductive material into sulfur as well as the formation of a stable framework. In this article, the structure of the **S-P3HT** copolymer and its composite with sulfur was studied in detail by various analytical tools, which confirmed the covalent linking between sulfur and P3HT. The use of **S-P3HT** in covalent linkage of sulfur composites led to an enhanced battery performance by effective stabilization of the electrodes during the operation of the battery. In addition, uniformly incorporated P3HT with sulfur can form a framework of successfully interconnected charge-transfer channels. This work clearly demonstrates that a homogeneous composite of **S-P3HT** and sulfur can be synthesized and assembled into electrodes for high-performance lithium−sulfur batteries.

EXPERIMENTAL SECTION

Materials. *tert*-Butylmagnesium chloride (tBuMgCl, 1.0 M in THF), allylmagnesium bromide (2.0 M in THF), [1,3-bis-(diphenylphosphino)propane]dichloronickel(II) (Ni(dppp)Cl_2), *N*-bromosuccinimide (NBS, 99%), and *o*-dichlorobenzene (DCB, 99%) were purchased from Sigma-Aldrich, and 3-hexylthiophene was purchased from TCI. NBS was recrystallized from water. All solvents were dried before use. Polyethylene binder (Sigma-Aldrich), conductive carbon (Super C65, Timcal), lithium bis-(trifluoromethane)sulfonimide (LiTFSI, Sigma-Aldrich), lithium nitrate ($LiNO_3$, Sigma-Aldrich), polypropylene separator (Celgard), lithium foil (FMC), 1,3-dioxolane (Novolyte), and 1,2-dimethoxyethane (Novolyte) were used as received.

Methods. *Synthesis of Allyl-Terminated P3HT.* The monomer 2,5-dibromo-3-hexylthiophene was synthesized according to literature.[25] Briefly, NBS (18.25 g, 98,7 mmol) was solved in DMF and added to a solution of 3-hexylthiophene (8.00 g, 47.7 mmol) in chloroform. The reaction was stirred under argon overnight at 60 °C. The reaction mixture was purified first by extracting with diethyl ether and then by column chromatography (petroleum ether; R_f of the product = 0.8). The yield of the colorless product was 71%.

^{1}H NMR (400 MHz, $CDCl_3$): δ [ppm] = 6.80 (s, 1H), 2.53 (t, J= 8.0 Hz, 2H), 1.57 (m, 1H), 1.34 (m, 6H), 0.92 (m, 3H).

The polymerization was conducted following a previous description.[26] 2,5-Dibromo-3-hexylthiophene (600 mg, 1,84 mmol), 4.2 mL of THF, and tBuMgCl (1.75 mmol) were stirred under argon for 20 h at room temperature. Afterward the reaction mixture was diluted with 9 mL of THF, and 25.6 mg of Ni(dppp)Cl_2 (0.05 mmol) was added to start the polymerization, whereupon the reaction mixture turned from slightly yellow to red. Allylmagnesium bromide (1.5 mmol) was added after 10 min, and the reaction mixture was stirred for a further 5 min. The polymer was precipitated in methanol. After centrifugation and drying, the polymer was purified by Soxhlet extraction using first methanol, then hexane, and finally chloroform. Typically, the yield was around 50%.

^{1}H NMR (400 MHz, $CDCl_3$): δ [ppm] = 7.01 (s, 31 H), 6.00 (m, 1H), 5.16 (m, 2H), 3.54 (d, J = 4.0 Hz 2H), 2.84 (bs, 62H), 1.74 (bs, 63H), 1.45−1.29 (bm, 192 H), 0.95 (bs, 96 H).

^{13}C NMR (400 MHz, $CDCl_3$): δ [ppm] = 140.0, 133.8, 136.5 (end-group), 130.6, 128.7, 116.3 (end-group), 32.3 (end-group), 31.9, 30.7, 29.6, 29.4, 22.8, 14.2.

SEC: M_n(P3HT) = 9450 g mol^{-1}, $Đ$ = 1.08.

Elemental analysis: Calculated for allyl-terminated P3HT: C, 72.29; H, 9.43; S, 19.28. Found: C, 71.86; H, 10.47; S, 17.67.

Synthesis of ***S-P3HT*** *Sulfur Composite.* Allyl-terminated P3HT was dissolved in DCB and added to an excess of sulfur, whereby the weight ratio between S and P3HT was varied (S:P3HT = 9.5:0.5, 9:1, 8:2). It should be noted that excess S was used to obtain the composite of **S-P3HT** and S. The reaction mixture was stirred for 1 h at 170 °C. After complete conversion as detected by NMR, the reaction mixture was quenched in methanol. After centrifugation, the product was dried under reduced pressure. The product can be obtained almost quantitatively.

^{1}H NMR (400 MHz, $CDCl_3$): δ [ppm] = 6.98 (s, 31 H), 3.2−3.8 (m), 2.80 (s, 62H), 1.74 (s, 63H), 1.45−1.20 (m, 192 H), 0.95 (s, 96H).

^{13}C NMR (400 MHz, $CDCl_3$): δ [ppm] = 140.0, 133.8, 130.6, 128.7, 120.0 (end-group) 31.9, 30.7, 29.6, 29.4, 29.1 (end-group), 22.8, 14.2.

SEC: M_n(S-P3HT) = 10 300 g mol^{-1}, $Đ$ = 1.13.

Elemental analysis: Found: C, 67.59; H, 9.43; S, 22.98.

Electrochemical Characterization. **S-P3HT** copolymer-containing compositions (**S-P3HT**/CB) were mixed with the binder (polyethylene) and conductive carbon (Super P) so that the mixture ratio was fixed to S:(P3HT+conductive carbon):polyethylene = 70:25:5. The **S-P3HT** mixtures were ball-milled for 30 min to pulverize and homogenize particles and then mixed with binder and carbon. Chloroform (2 mL) was added as a solvent. The slurry was casted on a current collector based on aluminum by doctor-blading method and dried under air. The sulfur loading was usually around 1 mg/cm^2. Reference electrodes containing S/P3HT/CB and S/CB were prepared in the same way with the same composition (i.e., S:(P3HT+conductive carbon):polyethylene = 70:25:5), and the sulfur loading was usually around 1 mg/cm^2 as well.

The prepared electrodes were used to assemble CR2032 coin cells in an argon-filled glovebox. The polyethylene separator was obtained from SK Innovation Corp. The electrolyte composition was 1.0 M LiTFSI and 0.1 M $LiNO_3$ in a 1:1 (v/v) mixture of 1,3-dioxolane and 1,2-dimethoxyethane (Panax Etec, Korea). Lithium foil was used as a counter electrode.

The electrochemical performance was evaluated by the use of a WBCS3000 battery tester (Won-A Tech, Korea) in a voltage range from 1.7 to 2.8 V vs Li^+/Li. Electrochemical impedance spectroscopy (EIS) measured at the charged state and the frequency range was fixed to 100 kHz to 10 mHz at the open circuit voltage (OCV). The AC amplitude was set to be 10 mV.

RESULTS AND DISCUSSION

The synthetic approach to obtain the **S-P3HT** copolymers is shown in Schemes 1 and 2. First, the conductive polymer used

Scheme 1. Synthesis of Allyl-Terminated P3HT Applying GRIM Polymerization

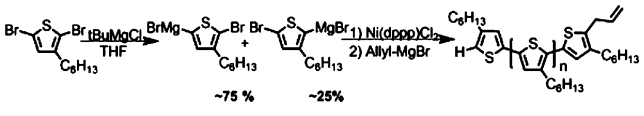

for the covalent incorporation into sulfur is synthesized by GRIM polymerization technique (see Scheme 1). This synthesis route allows the controlled synthesis of allyl-terminated P3HT. The monomer precursor 2,5-dibromo-3-hexylthiophene synthesized by bromination of the 3-hexylthiophene with NBS[25] is first treated with *tert*-butylmagnesium chloride (tBuMgCl), resulting in the Grignard metathesis

DOI: 10.1021/acs.chemmater.5b02317
Chem. Mater. XXXX, XXX, XXX−XXX

Scheme 2. (a) Synthetic Approach for the Copolymerization of Allyl-Terminated P3HT and Sulfur and (b) Proposed Microstructure of the Copolymer-Containing Sample

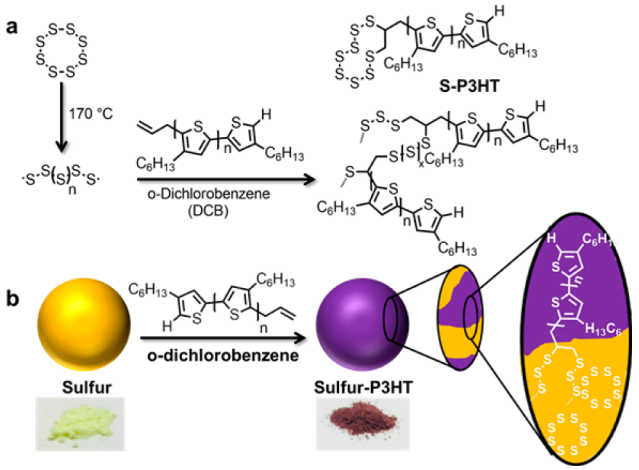

products with the magnesium species mainly incorporated on position 5 of the thiophene.[27,28] The reactive monomer is polymerized by the addition of Ni(dppp)Cl_2 as a catalyst.[27]

The polymer end-group functionalization is achieved by quenching of the polymerization with a second Grignard reagent, in this case with a solution of allylmagnesium bromide.[26,29] The allyl group first coordinates to the nickel catalyst and finally terminates the polymer by a reductive elimination reaction.[26] Matrix-assisted laser desorption/ionization time-of-flight mass spectroscopy (MALDI-TOF-MS) proves the successful incorporation of the allyl end-group, as the main peaks detected can be attributed to P3HT terminated with one H and one allyl end-group, as shown in Figure 1a. Besides the main peak a rather small peak can be identified as a Br/allyl-terminated P3HT.

^{1}H NMR spectroscopy further confirms the presence of the allyl end-group, as the typical allyl bands can be observed besides the typical broad peaks corresponding to the P3HT backbone and hexyl side-chains, as demonstrated in Figure 1b. Integration of the end-group signals and comparison with the backbone signal of the polymer at 6.99 ppm allow a rough estimation of the polymer chain length, and the average number of repeating units is determined to be around 30, assuming that all polymers are terminated with one allyl end-group (see Figure S1).

Heteronuclear single-quantum coherence (HSQC) NMR spectroscopy was conducted for the allyl-terminated polymer. As shown in Figure S2, the C/H couplings of the allyl end-group can be clearly identified.

According to size exclusion chromatography (SEC, Figure 1c), the polymer is rather monodispersed, with a polydispersity ($Đ$) of 1.08. The molecular weight (M_n) obtained by SEC is calculated to be 9450 g mol^{-1}, significantly higher than the value calculated by NMR spectroscopy (5022 g mol^{-1}). This is due to the stiff nature of P3HT, which leads to an overestimation of the molecular weight compared to the flexible polystyrene used for calibration of the SEC system.

The allyl end-group of the P3HT enables the reaction with sulfur radicals formed at elevated temperatures, which allows the covalent linkage of P3HT and sulfur (see Scheme 2). As the modified P3HT possesses only one allyl group, this reaction creates linear (soluble) polymers in which either a sulfur cycle is linked to the P3HT or several P3HT units are linked by sulfur bridges. As P3HT is not soluble in molten sulfur (see Figure 2), small amounts of DCB are added as a solvent. The

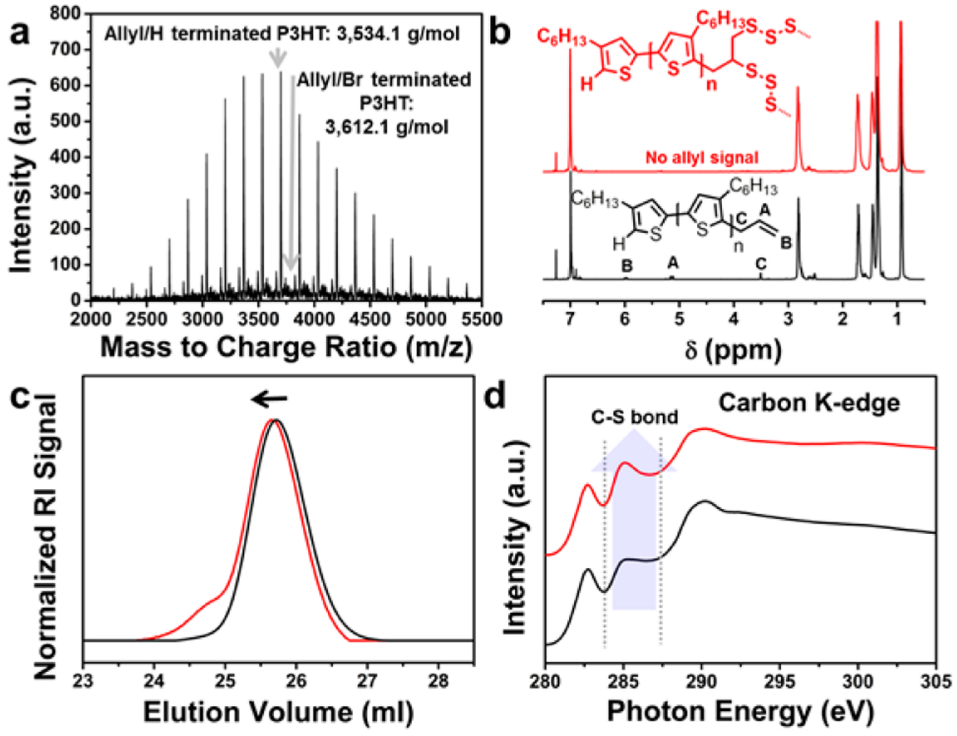

Figure 1. (a) MALDI-TOF spectrum of allyl-terminated P3HT. (b) NMR spectra, (c) SEC elugram, and (d) near-edge X-ray absorption fine structure spectra of the carbon K-edge, obtained using the 4 D beamline at the Pohang Light Source-II (3 GeV), of allyl-terminated P3HT (black) and **S-P3HT** copolymer (red).

DOI: 10.1021/acs.chemmater.5b02317
Chem. Mater. XXXX, XXX, XXX−XXX

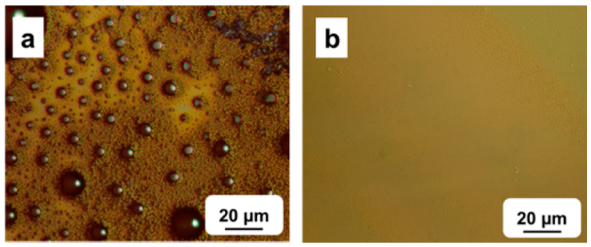

Figure 2. Optical microscopy images of a film obtained by drop-casting of (a) a mixture of sulfur and P3HT (not covalently linked) and (b) a mixture of sulfur and **S-P3HT** (8:2) copolymer. While the mixture of sulfur and P3HT shows severe phase separation, that of sulfur and **S-P3HT** forms a homogeneous and uniform film.

ratio between sulfur and P3HT was chosen to be S:P3HT = 9:1. The mixture was heated to 170 °C for the homolytic cleavage of the S_8 ring, to produce the sulfur radical species to initiate the reaction.

After the completion of the reaction (1 h), which was determined by ^{1}H NMR spectroscopy as the disappearance of the allyl double bond as shown in Figure 1b, the reaction mixture was quenched in methanol to precipitate **S-P3HT** sulfur composites consisting of **S-P3HT** in excess sulfur. NMR spectroscopy of **S-P3HT** further shows the presence of all previously observed aromatic backbone and aliphatic side-chain signals of P3HT, which confirms that no (significant) side reaction with the aromatic thiophene rings or aliphatic side chain occurs. Furthermore, the observed coupling signals of the allyl end-group disappear in the HSQC spectrum in the case of the **S-P3HT** copolymer, and instead two new coupling signals can be observed at 2.30/33.0 ppm and at 2.03/27.2 ppm (Figure S3), which fit to newly formed RCH_2-S and RR′CH-S groups. The SEC data shown in Figure 1c for the **S-P3HT** copolymer shows a shift to a lower elution volume compared to the allyl-terminated P3HT. This shift can be explained with the covalent linking of sulfur to the polymer, which increases the hydrodynamic radius of the P3HT polymer and lowers the elution volume. A shoulder at lower elution volumes, i.e., at higher molecular weight, might be attributed either to the connection of longer sulfur chains to the polymer or to the connection of P3HT polymer chains by sulfur bridges (Scheme 2a). However, the polydispersity of 1.13 is still rather low. To quantify the amount of incorporated sulfur within the **S-P3HT** copolymer, the excess sulfur was removed by preparative SEC. After the successful separation of the **S-P3HT** copolymer from the sulfur, elemental analysis was applied to allyl-terminated P3HT and compared to that of the **S-P3HT** copolymer. The copolymer has an increased sulfur content of about 5.3 wt.% compared to the allyl-terminated P3HT, corresponding to the addition of eight sulfur atoms on average per polymer chain, due to the radical reaction occurring between the double bond and sulfur radicals. This corresponds to the expectations according to the opening of a S_8 ring and the addition of the diradical to the olefinic double bond.

Soft X-ray absorption spectroscopy (XAS) (Pohang Light Source-II, 3 GeV) was also studied since XAS is a powerful tool for probing chemical bonding in the materials. Figure 1d represents the carbon K-edge absorption spectra for both the electrode containing **S-P3HT** copolymer and the electrode containing a mixture of P3HT and sulfur, in which sulfur and P3HT are not covalently linked with each other. Absorption features around 283 and 290 eV are observed in both samples. They are attributed to the π^* and σ^* states, respectively. Interestingly, the peak at ~285 eV results from C−S bonding nature and is significantly enhanced in the electrode with **S-P3HT** copolymer.[30] This indicates an enhanced chemical interaction between sulfur of S_8 and the carbon of P3HT since new C−S bonds are formed during the copolymerization. Raman spectroscopy was also performed to identify the C−S bonds in **S-P3HT** copolymer. In the Raman spectra shown in Figure S4, the typical bands of P3HT can be observed for the as-synthesized allyl-terminated P3HT. For **S-P3HT**, an additional band at 677 cm^{-1} can be observed, which can be attributed to the formation of new C−S bonds.

Because **S-P3HT** shall be used as an additive in sulfur batteries, miscibility between sulfur and **S-P3HT** (or P3HT) is of prime importance for the morphology of the electrode. Figure 2 shows optical microscopy images of films of allyl-terminated P3HT and **S-P3HT** with sulfur. While the system with a mixture of S and P3BT shows a distinct phase separation in the micrometric length scale, the mixture of **S-P3HT** and sulfur forms a smooth and homogeneous film, which confirms that the copolymer can be well dispersed in sulfur.

The homogeneous incorporation of **S-P3HT** into sulfur is further proven by scanning electron microscopy (SEM) and energy-dispersive X-ray spectroscopy (EDX) of **S-P3HT** composites (used for the preparation of sulfur batteries later). EDX measurements (Figure 3) show that the carbon signal in

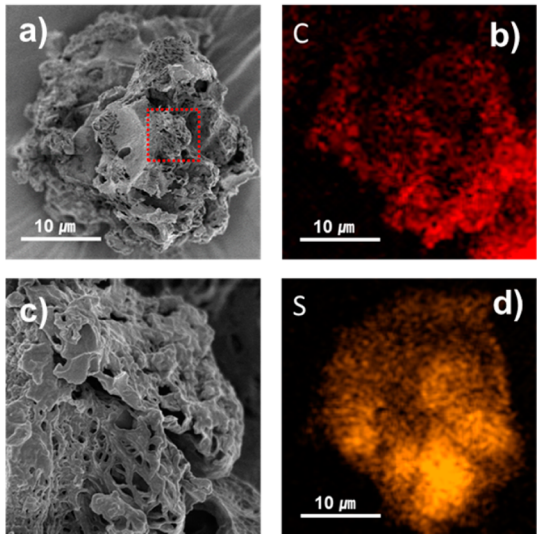

Figure 3. SEM image and EDX analysis of **S-P3HT** sulfur composites (8:2), showing SEM images with low (a) and high (c) magnification and corresponding elemental mapping of C (b) and S (d) of the particle in the red box in (a).

the elemental mapping is well dispersed within the particle. As sulfur and P3HT by themselves are not miscible, we assume that the long sulfur bridges and cycles (on average S_8) in **S-P3HT** dissolve in the sulfur matrix. This leads to a reduction of the crystallinity in the elementary sulfur (XRD measurements, Figure S6). In this way, **S-P3HT** decorated with sulfur chains acts as a polymeric surfactant, which forms nanometer-sized phase-separated structures of P3HT within the sulfur (as shown schematically in Scheme 2b).

Thermogravimetric analysis (TGA) of the composite S/**S-P3HT** (which contains excess sulfur and the **S-P3HT** copolymer) was conducted under a nitrogen atmosphere.

DOI: 10.1021/acs.chemmater.5b02317
Chem. Mater. XXXX, XXX, XXX−XXX

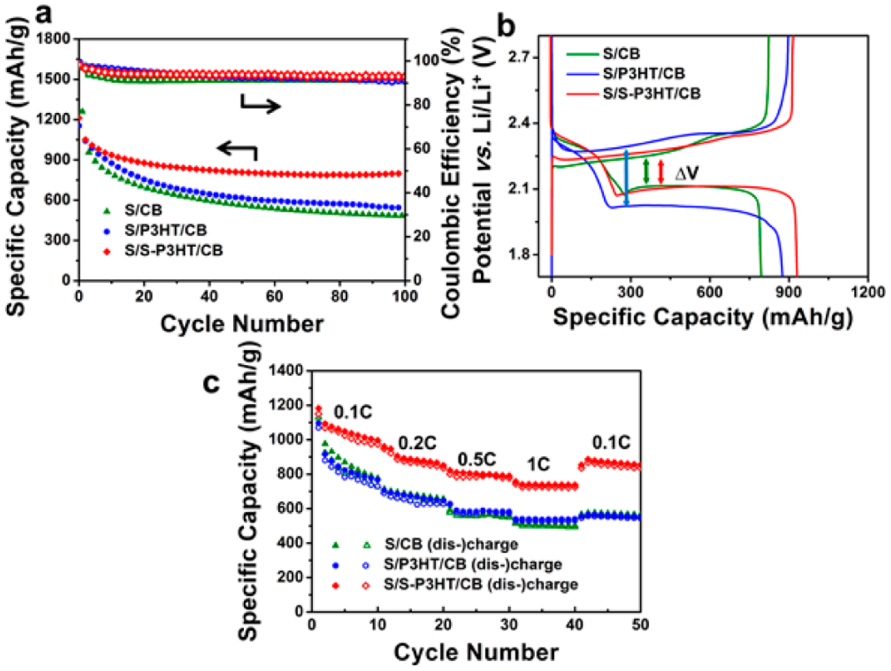

Figure 4. (a) Cycling performance, (b) capacity vs voltage profiles of the 10th cycle, and (c) C-rate performance of S/CB (green), S/P3HT/CB (blue), and S/**S-P3HT**/CB (red).

The detected weight loss at 280 °C (see Figure S5) is attributed to the evaporation of sulfur and is in good agreement with the amount of sulfur added for the synthesis, which was 86 wt.%. Generally, it is also possible to vary the ratio between sulfur and P3HT during the copolymerization, and exemplarily further ratios between S and P3HT were chosen, such as S:P3HT = 9.5:0.5 and 8:2 (see photo in Figure S5). The weight loss detected by TGA in these cases is 93 and 79 wt.%, respectively (Figure S5). The decomposition temperatures of **S-P3HT** copolymers are very similar to that of pure sulfur. This is ascribed to the presence of elementary sulfur in the S/**S-P3HT** composite, which is not directly connected with P3HT.

Since the majority of sulfur in the composite is elemental and not bound to the P3HT, it exhibits the same vaporization temperature with pure sulfur. After vaporization of elemental sulfur in **S-P3HT** at 300 °C, residual sulfur that is bound to P3HT, i.e., S in **S-P3HT**, shows gradual thermal decomposition, as can be seen as a gentle slope. It is also noteworthy that P3HT itself shows thermal decomposition at 500 °C; however, **S-P3HT** copolymers do not decompose up to 700 °C. Such thermal stabilization of P3HT has been reported in other composite systems,[31] which further supports the strong interaction between sulfur and P3HT in **S-P3HT**.

In order to investigate the significance of the finely dispersed **S-P3HT** on the battery performance of sulfur particles, three different electrodes were applied as a cathode material: (i) sulfur and carbon black (S/CB); (ii) sulfur, P3HT, and CB (S/P3HT/CB); and (iii) sulfur, **S-P3HT**, and CB (S/**S-P3HT**/CB). They were thoroughly mixed to prepare the cathode electrode. In all electrodes, the amount of conductive material, i.e., the sum of carbon black and P3HT, was set to be 25 wt.%. As shown in the galvanostatic cycling experiment in Figure 4a, initial specific capacities of S/CB, S/P3HT/CB, and S/**S-P3HT**/CB were 1260, 1154, and 1212 mAh g^{-1} at 0.5C (1C is defined as 1675 mA g^{-1}), respectively. A slightly higher initial capacity of S/CB can be achieved due to the higher electrical conductivity of CB than P3HT. However, as cycles go on, the system S/**S-P3HT**/CB exhibits a superior cycling performance compared with S/CB and S/P3HT/CB. S/CB and S/P3HT/CB electrodes show a rapid drop of capacity within the first 20 cycles to 696 and 754 mAh g^{-1}, respectively. In contrast, the capacity of S/**S-P3HT**/CB is 877 mAh/g after 20 cycles and is preserved with very little decay upon further cycling. The capacity of S/**S-P3HT**/CB is still conserved after 100 cycles at 799 mAh g^{-1}, compared to 482 and 544 mAh g^{-1} for S/CB and S/P3HT/CB, respectively.

From the electrochemical performance, it seems that the homogeneous incorporation of P3HT into sulfur (as schematically shown in Scheme 2 and proven in Figures 2 and 3) can stabilize the electrode against irreversible loss of polysulfides during the repeated cycles. From this perspective, a strong molecular interaction between Li_xS_n and P3HT should exist. Li et al. also reported a strong interaction between heteroatoms and Li_xS_n in conjugated polymers, which was claimed to be responsible for the low loss of active material in their model systems, leading to the enhanced battery performance.[32] Additionally, Guo et al. suggested an interaction between nitrogen and lithium ions in a thermally obtained conjugated polymer.[20] It is expected that such an interaction can exist even in S/P3HT/CB; however, this interaction can be limited due to the small interface, as can be seen in Figure 2. This might explain the slightly enhanced capacities of S/P3HT/CB compared to S/CB. However, the good dispersibility of P3HT units in the sulfur matrix, as achieved with S/**S-P3HT**/CB, facilitates interaction due to the large interface, resulting in good capacity retention. This capacity retention can be even further improved by increasing the amount of **S-P3HT** copolymer in the composite, e.g., by adding more allyl-terminated P3HT during copolymerization. Figure S7 shows the results for a **S-P3HT** composite synthesized with a weight ratio S:P3HT = 8:2. Here a capacity of 838 mAh g^{-1} can be obtained after 100 cycles. Meanwhile, the sample consisting of

DOI: 10.1021/acs.chemmater.5b02317
Chem. Mater. XXXX, XXX, XXX−XXX

the more conductive CB (i.e., S/CB) features a higher initial capacity but exhibits a higher loss of active material upon cycling (see the first cycle and the rest of the cycles in galvanostatic cycling, Figure 4a) since S/CB is prone to the loss of polysulfides.

Figure 4b displays the charge/discharge profiles of all three systems after 10 cycles, which can provide information about the overpotential of each sample. The overpotential can be determined from the potential difference between the discharge and charge plateaus (see arrows in Figure 4b). While S/P3HT/CB exhibits a severe increase of overpotential, the S/**S-P3HT**/CB electrode shows an overpotential similar to that of S/CB. The increase of the S/P3HT/CB overpotential compared with those of S/CB and S/**S-P3HT**/CB can result from the increase of resistance due to (i) the lower conductivity of P3HT (compared to CB) and (ii) an increased interfacial resistance between sulfur and P3HT in the macroscopically separated sample (see Figure 1). The similar overpotentials of S/**S-P3HT**/CB and S/CB show that the lower conductivity of P3HT units can be compensated by the homogeneous incorporation of P3HT into the composite at the nanoscale dimension.

EIS data also confirm the charge-transfer kinetics among the electrodes, as shown in Figure S8. The semicircle on the Z_{re} axis, corresponding to the charge-transfer resistance, is the smallest for S/**S-P3HT**/CB, whereas the semicircle for S/P3HT/CB is significantly larger. Thus, S/**S-P3HT**/CB has the highest conductivity (lowest resistance). As a result, besides the advantage of trapping polysulfides, the homogeneous incorporation of P3HT results in a decreased charge-transfer resistance, which contributes to the enhancement of the battery performance as well. It should be noted that the S/P3HT/CB electrode showed a decrease of charge transfer as cycles proceeded, while S/CB- and **S-P3HT**-based electrodes did not show a change during the cycles. The decrease of charge transfer is well known in Li−S batteries, as reported elsewhere.[33] At the initial stage, sulfur, P3HT, and CB are macroscopically segregated; however, such inhomogeneous distribution changes upon cycling because of rearrangement of the structure. During the discharge process of S_8, S_8 transforms to the liquid phase by formation of high-order polysulfides. Afterward, high-order polysulfides transform back to the solid phases of low-order polysulfides as Li_2S. Such successive transformations between solid and liquid phases bring about the rearrangement of structures which are totally different from those in the initial stage and more favorable for the reaction. In general, the change of charge transfer is not prominent. However, in the case of S/P3HT/CB, the decrease of charge transfer is clearly observed due to their structural disintegrity or inhomogeneity at the initial stage.

Furthermore, the S/**S-P3HT**/CB electrode exhibits a superior C-rate capability, as shown in Figure 4c. Significantly higher specific capacities can be obtained for all applied currents in the case of S/**S-P3HT**/CB; 739.41 mAh g^{-1} at 1C was obtained in the S/**S-P3HT**/CB, whereas S/P3HT/CB and S/CB electrodes revealed lower capacities of 527 and 501 mAh g^{-1}, respectively. The structural integrity at the nano and mesoscale of S/**S-P3HT**/CB accounts for the enhancement of the rate capability by the shortened diffusion length of the reactant.

CONCLUSIONS

Copolymerization of allyl-terminated P3HT with sulfur is possible by a radical reaction between the allyl end-group and diradical sulfur species. This approach allows the covalent linkage of long sulfur chains to allyl-terminated P3HT and creates a copolymer with one segment compatible with elementary sulfur and the other segment compatible with P3HT, which allows fine and homogeneous dispersion (submicrometer range) of P3HT into a sulfur matrix. The homogeneous incorporation of this semiconducting polymer into sulfur particles features two effects: (i) it lowers the loss of active material due to the strong interaction between the polysulfides and the polythiophene, and (ii) it lowers the electrical resistance. Thus, an improved battery performance can be achieved by using **S-P3HT** copolymers in combination with sulfur particles. The direct evidence of the interaction between **S-P3HT** and polysulfides will be studied using *in situ* local structure probing tools such as X-ray absorption, NMR, etc. Furthermore, detailed morphological observations using various analytical tools will be studied to further improve the battery performance.

ASSOCIATED CONTENT

Supporting Information

The Supporting Information is available free of charge on the ACS Publications website at DOI: 10.1021/acs.chemmater.5b02317.

Figures S1−S8, showing NMR, HSQC, Raman, and electrochemical impedance spectra, TGA data, and additional galvanostatic cycling data (PDF)

AUTHOR INFORMATION

Corresponding Authors

* E-mail: ysung@snu.ac.kr (Y.-E.S.).
*E-mail: zentel@uni-mainz.de (R.Z.).

Author Contributions

#B.O. and J.P. contributed equally.

Notes

The authors declare no competing financial interest.

ACKNOWLEDGMENTS

B.O. thanks the Graduate School in Mainz and is the recipient of a fellowship through the Excellence Initiative (DFG/GSC 266). This work was supported by the Institute for Basic Science (IBS-R006-G1), Republic of Korea, and the IRTG 1404, jointly funded by DFG and NRF.

REFERENCES

(1) Armand, M.; Tarascon, J.-M. Building Better Batteries. *Nature* **2008**, *451*, 652−657.

(2) Bresser, D.; Passerini, S.; Scrosati, B. Recent Progress and Remaining Challenges in Sulfur-Based Lithium Secondary Batteries - a Review. *Chem. Commun.* **2013**, *49*, 10545.

(3) Evers, S.; Nazar, L. F. New Approaches for High Energy Density Lithium-Sulfur Battery Cathodes. *Acc. Chem. Res.* **2013**, *46*, 1135−1143.

(4) Bruce, P. G.; Freunberger, S. A.; Hardwick, L. J.; Tarascon, J.-M. LiO_2 and Li-S Batteries with High Energy Storage. *Nat. Mater.* **2011**, *11*, 19−29.

(5) Mikhaylik, Y. V.; Akridge, J. R. Polysulfide Shuttle Study in the Li/S Battery System. *J. Electrochem. Soc.* **2004**, *151*, A1969−A1976.

DOI: 10.1021/acs.chemmater.5b02317
Chem. Mater. XXXX, XXX, XXX−XXX

(6) Manthiram, A.; Fu, Y.; Su, Y.-S. Challenges and Prospects of Lithium-Sulfur Batteries. *Acc. Chem. Res.* **2013**, *46*, 1125−1134.
(7) Yang, Y.; Yu, G.; Cha, J. J.; Wu, H.; Vosgueritchian, M.; Yao, Y.; Bao, Z.; Cui, Y. Improving the Performance of Lithium–Sulfur Batteries by Conductive Polymer Coating. *ACS Nano* **2011**, *5*, 9187−9193.
(8) Wang, J.; Yang, J.; Xie, J.; Xu, N. A Novel Conductive Polymer-Sulfur Composite Cathode Material for Rechargeable Lithium Batteries. *Adv. Mater.* **2002**, *14*, 963−965.
(9) Wu, F.; Chen, J.; Chen, R.; Wu, S.; Li, L.; Chen, S.; Zhao, T. Sulfur/Polythiophene with a Core/Shell Structure: Synthesis and Electrochemical Properties of the Cathode for Rechargeable Lithium Batteries. *J. Phys. Chem. C* **2011**, *115*, 6057−6063.
(10) He, G.; Ji, X.; Nazar, L. High ″C″ Rate Li-S Cathodes: Sulfur Imbibed Bimodal Porous Carbons. *Energy Environ. Sci.* **2011**, *4*, 2878.
(11) Ji, X.; Lee, K. T.; Nazar, L. F. A highly Ordered Nanostructured Carbon-Sulphur Cathode for Lithium-Sulphur Batteries. *Nat. Mater.* **2009**, *8*, 500−506.
(12) Zheng, G.; Yang, Y.; Cha, J. J.; Hong, S. S.; Cui, Y. Hollow Carbon Nanofiber-Encapsulated Sulfur Cathodes for High Specific Capacity Rechargeable Lithium Batteries. *Nano Lett.* **2011**, *11*, 4462−4467.
(13) Cao, Y.; Li, X.; Aksay, I. A.; Lemmon, J.; Nie, Z.; Yang, Z.; Liu. Sandwich-Type Functionalized Graphene Sheet-Sulfur Nanocomposite for Rechargeable Lithium Batteries. *Phys. Chem. Chem. Phys.* **2011**, *13*, 7660.
(14) Evers, S.; Nazar, L. F. Graphene-Enveloped Sulfur in a One Pot Reaction: a Cathode with Good Coulombic Efficiency and High Practical Sulfur Content. *Chem. Commun.* **2012**, *48*, 1233.
(15) Zhang, D.; Tu, J. P.; Xiang, J. Y.; Qiao, Y. Q.; Xia, X. H.; Wang, X. L.; Gu, C. D. Influence of Particle Size on Electrochemical Performances of Pyrite FeS_2 for Li-Ion Batteries. *Electrochim. Acta* **2011**, *56*, 9980−9985.
(16) Wang, J.-Z.; Lu, L.; Choucair, M.; Stride, J. A.; Xu, X.; Liu, H.-K. Sulfur-Graphene Composite for Rechargeable Lithium Batteries. *J. Power Sources* **2011**, *196*, 7030−7034.
(17) Moon, J.; Park, J.; Jeon, C.; Lee, J.; Jo, I.; Yu, S.-H.; Cho, S.-P.; Sung, Y.-E.; Hong, B. H. An Electrochemical Approach to Graphene Oxide Coated Sulfur for Long Cycle Life. *Nanoscale* **2015**, *7*, 13249−13255.
(18) Seh, Z. W.; Zhang, Q.; Li, W.; Zheng, G.; Yao, H.; Cui, Y. Stable Cycling of Lithium Sulfide Cathodes through Strong Affinity with a Bifunctional Binder. *Chem. Sci.* **2013**, *4*, 3673.
(19) Ma, L.; Zhuang, H.; Lu, Y.; Moganty, S. S.; Hennig, R. G.; Archer, L. A. Tethered Molecular Sorbents: Enabling Metal-Sulfur Battery Cathodes. *Adv. Energy Mater.* **2014**, *4*, 1400390.
(20) Guo, J.; Yang, Z.; Yu, Y.; Abruña, H. D.; Archer, L. A. Lithium-Sulfur Battery Cathode Enabled by Lithium-Nitrile Interaction. *J. Am. Chem. Soc.* **2013**, *135*, 763−767.
(21) Chung, W. J.; Griebel, J. J.; Kim, E. T.; Yoon, H.; Simmonds, A. G.; Ji, H. J.; Dirlam, P. T.; Glass, R. S.; Wie, J. J.; Nguyen, N. A.; Guralnick, B. W.; Park, J.; Somogyi, Á.; Theato, P.; Mackay, M. E.; Sung, Y.-E.; Char, K.; Pyun, J. The Use of Elemental Sulfur as an Alternative Feedstock for Polymeric Materials. *Nat. Chem.* **2013**, *5*, 518−524.
(22) Simmonds, A. G.; Griebel, J. J.; Park, J.; Kim, K. R.; Chung, W. J.; Oleshko, V. P.; Kim, J.; Kim, E. T.; Glass, R. S.; Soles, C. L.; Sung, Y.-E.; Char, K.; Pyun, J. Inverse Vulcanization of Elemental Sulfur to Prepare Polymeric Electrode Materials for Li-S Batteries. *ACS Macro Lett.* **2014**, *3*, 229−232.
(23) Dirlam, P. T.; Simmonds, A. G.; Kleine, T. S.; Nguyen, N. A.; Anderson, L. E.; Klever, A. O.; Florian, A.; Costanzo, P. J.; Theato, P.; Mackay, M. E.; Glass, R. S.; Char, K.; Pyun, J. Inverse Vulcanization of Elemental Sulfur with 1,4-diphenylbutadiyne for Cathode Materials in Li–S Batteries. *RSC Adv.* **2015**, *5*, 24718−24722.
(24) Dirlam, P. T.; Simmonds, A. G.; Shallcross, R. C.; Arrington, K. J.; Chung, W. J.; Griebel, J. J.; Hill, L. J.; Glass, R. S.; Char, K.; Pyun, J. Improving the Charge Conductance of Elemental Sulfur via Tandem Inverse Vulcanization and Electropolymerization. *ACS Macro Lett.* **2015**, *4*, 111−114.
(25) Nie, Y.; Zhao, B.; Tang, P.; Jiang, P.; Tian, Z.; Shen, P.; Tan, S. Synthesis and Photovoltaic Properties of Copolymers based on Benzo[1,2-b:4,5-b]dithiophene and Thiophene with Electron-Withdrawing Side Chains. *J. Polym. Sci., Part A: Polym. Chem.* **2011**, *49*, 3604−3614.
(26) Jeffries-EL, M.; Sauvé, G.; McCullough, R. D. Facile Synthesis of End-Functionalized Regioregular Poly(3-alkylthiophene)s via Modified Grignard Metathesis Reaction. *Macromolecules* **2005**, *38*, 10346−10352.
(27) Loewe, R. S.; Khersonsky, S. M.; McCullough, R. D. A Simple Method to Prepare Head-to-Tail Coupled, Regioregular Poly(3-alkylthiophenes) Using Grignard Metathesis. *Adv. Mater.* **1999**, *11*, 250−253.
(28) Loewe, R. S.; Ewbank, P. C.; Liu, J.; Zhai, L.; McCullough, R. D. Regioregular, Head-to-Tail Coupled Poly(3-alkylthiophenes) Made Easy by the GRIM Method: Investigation of the Reaction and the Origin of Regioselectivity. *Macromolecules* **2001**, *34*, 4324−4333.
(29) Jeffries-EL, M.; Sauvé, G.; McCullough, R. D. In-Situ End-Group Functionalization of Regioregular Poly(3-alkylthiophene) Using the Grignard Metathesis Polymerization Method. *Adv. Mater.* **2004**, *16*, 1017−1019.
(30) Stöhr, J. *NEXAFS Spectroscopy*; Springer Series in Surface Sciences *25*; Springer: Berlin/Heidelberg, 1992.
(31) Peng, Y.; Song, G.; Hu, X.; He, G.; Chen, Z.; Xu, X.; Hu, J. In Situ Synthesis of P3HT-Capped CdSe Superstructures and their Application in Solar Cells. *Nanoscale Res. Lett.* **2013**, *8*, 106.
(32) Li, W.; Zhang, Q.; Zheng, G.; Seh, Z. W.; Yao, H.; Cui, Y. Understanding the Role of Different Conductive Polymers in Improving the Nanostructured Sulfur Cathode Performance. *Nano Lett.* **2013**, *13*, 5534−5540.
(33) Cañas, N. A.; Hirose, K.; Pascucci, B.; Wagner, N.; Friedrich, K. A.; Hiesgen, R. Investigations of Lithium−Sulfur Batteries using Electrochemical Impedance Spectroscopy. *Electrochim. Acta* **2013**, *97*, 42−51.

DOI: 10.1021/acs.chemmater.5b02317
Chem. Mater. XXXX, XXX, XXX−XXX